



1 Vertical profiles of sub-3 nm particles over the boreal forest

2

3 Katri Leino^{1*}, Janne Lampilahti¹, Pyry Poutanen¹, Riikka Väänänen¹, Antti Manninen¹, Stephany
4 Buenrostro Mazon¹, Lubna Dada¹, Anna Nikandrova¹, Daniela Wimmer¹, Pasi P. Aalto¹, Lauri R.
5 Ahonen¹, Joonas Enroth¹, Juha Kangasluoma¹, Petri Keronen¹, Frans Korhonen¹, Heikki Laakso¹,
6 Teemu Matilainen¹, Erkki Siivola¹, Hanna E. Manninen^{1,2}, Katrianne Lehtipalo¹, Veli-Matti
7 Kerminen¹, Tuukka Petäjä¹ and Markku Kulmala¹

8 ¹ Institute for Atmospheric and Earth System Research / Physics, Faculty of Science, P.O. Box 64, FI-00014 University
9 of Helsinki, Finland

10 (* corresponding author's email: katri.e.leino@helsinki.fi)

11 ²CERN, CH-1211 Geneva 23, Switzerland.

12 **Abstract.** This work presents airborne observations of sub-3 nm particles in the lower troposphere
13 and investigates new particle formation (NPF) within an evolving boundary layer (BL). We studied
14 particle concentrations together with supporting gas and meteorological data inside the planetary BL
15 over a boreal forest site in Hyytiälä, Southern Finland. The analysed data were collected during three
16 flight measurement campaigns: May-June 2015, August 2015 and April-May 2017, including 27
17 morning and 26 afternoon vertical profiles. As a platform for the instrumentation, we used a Cessna
18 172 aircraft. The analysed flight data were collected horizontally within a 30-km distance from the
19 SMEAR II station in Hyytiälä and vertically from 100 m above ground level up to 2700 m. The
20 number concentration of 1.5–3 nm particles was observed to be, on average, the highest near the
21 forest canopy top and to decrease with an increasing altitude during the mornings of NPF event days.
22 This indicates that the precursor vapours emitted by the forest play a key role in NPF in Hyytiälä.
23 During daytime, newly-formed particles were observed to grow in size and the particle population
24 became more homogenous within the well-mixed BL in the afternoon. During undefined days in
25 respect to NPF, we also detected an increase in concentration of 1.5–3 nm particles in the morning
26 but not their growth in size, which indicates an interrupted NPF process during these undefined days.
27 Vertical mixing was typically stronger during the NPF event days than during the undefined or non-
28 event days.

29



30 1 Introduction

31

32 One of the most important sources of secondary aerosol particles in the atmosphere is new particle
33 formation (NPF). NPF and subsequent growth is a globally observed phenomenon (Kulmala et al.,
34 2004; Kulmala and Kerminen, 2008; Kerminen et al., 2018). It is still partly unclear where, when and
35 how NPF occurs in the atmosphere. Aerosol measurements on board of an aircraft can give
36 information about the vertical, horizontal and spatial extent of the NPF in the lower atmosphere.

37 The planetary boundary layer (PBL) is a complex layer in the lowest part of the atmosphere, defined
38 as the part of the troposphere that is directly connected to the Earth's surface through the exchange
39 of momentum, heat and mass, and responds to surface forcing with a timescale of an hour or less
40 (Stull, 2012). The PBL has a characteristic diurnal cycle, but the detailed development varies from
41 day to day. Several meteorological, physical and chemical processes influence the spatial and
42 temporal conditions inside the BL, such as the boundary layer height (BLH) and mixing strength.
43 This gives rise to the complexity to define the exact BLH or to characterize the typical BL structure
44 or height at a given location.

45 Several airborne measurements have been conducted to investigate particle number concentrations
46 and size distributions as well as NPF inside the PBL. Over Europe, Crumeyrolle et al. (2010) observed
47 that the horizontal extent of NPF was about 100 km or larger during the EUCAARI campaign in 2008
48 (Kerminen et al., 2010), while Wehner et al. (2007) estimated a corresponding scale of up to 400 km
49 with clear horizontal variability in NPF characteristics during the SATURN campaign in 2002. The
50 number concentrations and size distributions of naturally charged particles (air ions) were under
51 investigation during EUCAARI-LONGREX campaign in May 2008 (Mirme et al., 2010). They
52 reported that NPF takes place throughout the whole BL, and that the particles have formed more
53 likely via neutral than ion-induced pathways inside the PBL.

54 In addition to NPF near to the surface inside the PBL and NPF in the free troposphere (FT) (Bianchi
55 et al., 2016), NPF has also been observed near clouds (Wehner et al., 2015). Siebert et al. (2004) and
56 Platis et al. (2016) observed NPF to initiate on top of the boundary layer in a capping inversion
57 followed by subsequent mixing of the freshly formed particles throughout the well-mixed boundary
58 layer. Similar observations were reported by Chen et al. (2017). Wehner et al. (2010) studied NPF in
59 the residual layer and observed that turbulent mixing is likely to lead to a local super saturation of



60 possible precursor gases, which is essential for NPF. The particles were formed in parts of the residual
61 layer and subsequently entrained into the BL where they were detected at the surface.

62 NPF events are frequently occurring over the boreal forest region in Southern Finland (Kulmala et
63 al., 2001; Dal Maso et al., 2005; Kulmala et al., 2013). In addition to ground-based measurements at
64 the SMEAR II station (61°51'N, 24°17'E, 181 m above sea level, Hari and Kulmala, 2005), which
65 have been conducted continuously since 1996, also airborne measurements of aerosol particles have
66 been carried out near the station since the year 2003 during several campaigns using a small aircraft
67 (O'Dowd et al., 2009; Schobesberger et al., 2013; Väänänen et al., 2016) and a hot-air balloon
68 (Laakso et al., 2007). Laakso et al. (2007) observed NPF to occur in the mixed BL, but also in the FT
69 with no connection to the BL nucleation. O'Dowd et al. (2009) observed NPF throughout the BL over
70 the SMEAR II, with the nucleation mode number concentration peaking first above the forest canopy.
71 Schobesberger et al. (2013) observed NPF inside the PBL. High concentrations of nucleation mode
72 particles were also found in the upper parts of the PBL, which indicates that nucleation does not
73 necessarily occur only close to the surface. Väänänen et al. (2016) studied the vertical and horizontal
74 extent of NPF in the lower troposphere near to the SMEAR II station. They observed that the air
75 masses within 30 km from SMEAR II differed only slightly from the ground-based observations at
76 the station, although the variability was larger for nucleation mode particles than for larger particles.
77 Furthermore, Väänänen et al. (2016) detected NPF to take place both inside the BL and, occasionally,
78 in the FT.

79 One of the sinks of newly formed aerosol particles in the PBL is dry deposition, which is important
80 especially for the smallest particles (Rannik et al., 2000; Lauros et al., 2011). Recently, Zha et al.
81 (2017) studied the vertical profile of highly oxygenated organic compounds (HOMs), which are
82 known precursors for aerosol formation (Ehn et al., 2014). They found that while the concentrations
83 were similar below and above canopy (35 m) during well-mixed conditions, the concentrations were
84 often clearly lower near the ground level during night-time, when temperature inversion occurred,
85 probably due to changes in their sources and sinks (e.g. surface deposition) during stable conditions.

86 In this study, we investigate the vertical variation of 1.5–3 nm and 3–10 nm particles from the ground
87 level up to 3 kilometres during different kind of days in relation to the occurrence of NPF at the
88 ground level, as well as the vertical mixing of a particle population within the evolving BL. The
89 dataset was collected during three measurement flight campaigns, in spring 2015, August 2015 and
90 in spring 2017, within a 30-km distance from the SMEAR II station. The results are compared to the



91 data measured on the ground level at the station. Traditional NPF event classification is used to
92 classify studied days as NPF events, non-events and undefined days (Dal Maso et al., 2005).

93 The questions we would like to answer are: Which kind of characteristics do we have in the vertical
94 profile of small particles?; How do these profiles differ between the NPF event, non-event and
95 undefined days?; Where do new particles form and how does the strength of turbulent mixing affect
96 particle concentrations?; What is the median concentration of small particles inside the BL during the
97 NPF event, non-event and undefined days, and how well do the results agree with the values measured
98 on the ground level?

99

100 **2 Materials and methods**

101 **2.1 Measurements on board Cessna**

102 As a platform for aerosol instruments, we used a light one-engine Cessna FR172F aircraft. The
103 measurement instruments were installed on an aluminium rack at the middle part inside the plane's
104 cabin (Fig. 1). A steel inlet line (with 32 mm inner diameter) was mounted onto the top of the rack
105 and lifted in and out from the window in the left side of the plane. The sample was collected from a
106 50-cm distance from the fuselage of the plane. The main flow in the steel tube was kept constant at
107 47 l min^{-1} during the measurement flight and was produced by suction in the venturi and forward
108 motion of the airplane. Each instrument took their actual inlet flow from the central line of the main
109 flow, minimizing the diffusional losses of the smallest particles. The measurements were performed
110 with an airspeed of 125 km/h. More details about partly the same instrumentation and layout can be
111 found in Schobesberger et al. (2013) and Väänänen et al. (2016). The data were collected within a
112 30-km distance from SMEAR II station and the area is covered mainly by coniferous forest.

113 **2.1.1 Instrumentation**

114 The main instrumentation for this study consisted of several different particle counters. An ultrafine
115 condensation particle counter (uCPC, model TSI-3776) is an instrument that detects the total
116 concentration of particles larger than about 3 nm in diameter. Particles larger than the threshold
117 diameter are grown into large droplets by condensing butanol vapour onto their surface, after which
118 they are detected optically with a laser-diode photodetector. The ultrafine CPC has an internal vacuum
119 pump that draws the aerosol sample with flow rate of 1.5 l min^{-1} into the instrument.



120 Airmodus Ltd has developed a mixing-type Particle Size Magnifier (PSM). The instrument is able to
121 detect directly sub-3 nm atmospheric particles using diethylene glycol (DEG) as condensing fluid
122 (Vanhanen et al., 2011). Compared with typically-used working fluids in CPCs, water and butanol,
123 the advantages of using DEG as condensing fluid are its lower saturation vapour pressure and higher
124 surface tension, which enables to detect particles down to 1 nm. The PSM requires a separate water
125 or butanol counter (CPC) for detecting optically the grown particles. The PSM in this study was a
126 model A10, operating with a butanol CPC (model TSI-3010). During the flight measurements
127 presented here, the instrument was used in fixed saturator flow rate mode measuring the total particle
128 concentration with a 1.5 nm cut-off size.

129 The instrumentation included also a custom-built Scanning Mobility Particle Sizer (SMPS), which
130 measures the particle number size distribution in the diameter size range of 10–400 nm with a 2-min
131 time resolution. Before the classification of an aerosol population, the particles are transported to a
132 radioactive source where they reach a constant bipolar charge equilibrium. The SMPS contains a
133 differential mobility analyser (DMA, Hauke type), while particle number concentrations are
134 measured with a butanol CPC (model TSI-3010).

135 The concentrations of water vapour (H₂O) and carbon dioxide (CO₂) were measured with a Li-Cor
136 (LI-840) gas analyser located in the instrumentation rack. Basic meteorological variables, including
137 the ambient temperature, relative humidity (RH) and static pressure, were measured. Pressure was
138 measured inside the plane while the temperature and RH sensor was located in the right wing of the
139 plane. The location of plane was recorded by a GPS receiver.

140 **2.2 SMEAR II research station**

141 A research Station for Measuring Ecosystem-Atmospheric Relations (SMEAR) II in Hyytiälä,
142 Southern Finland, was established in 1995 (see Hari and Kulmala, 2005). The station is equipped
143 with several aerosol and gas instruments together with flux, irradiation and meteorological
144 measurements. The long-term measurements give reliable and comprehensive knowledge about
145 ambient conditions at a relatively clean coniferous forest site. The station includes ground-based
146 measurements, tower measurements at the 35-m height above the ground level right above the
147 canopy, and measurements conducted from a mast at different altitudes up to 128 m.

148 In this study, we mainly used particle data from the ground level as a reference data to which we
149 compare our flight measurement data. The number concentrations in the size range of 1.5–3 nm were
150 calculated from the difference between the measured total particle concentration at 1.5 nm cut-off



151 size (from the PSM) and total concentration at 3 nm cut-off size (from DMPS). The distance between
152 the PSM and DMPS is vertically a few meters and horizontally a few tens of meters, which causes
153 some uncertainties in 1.5–3 nm particle number concentrations, especially during poorly-mixed BL
154 times in the morning when the two instruments do not always measure the same air mass.

155 The sensible heat flux (SHF) was measured at the at 23-m height, and we used these data to get
156 qualitative information on the strength of vertical mixing in the measured air masses.

157 **2.3 Data analysis**

158 The particle number concentration in size range of 1.5–3 nm was calculated as the difference of the
159 total particle concentrations measured with the PSM and uCPC on board the Cessna. The cut-off sizes
160 of these instruments were 1.5 nm and 3 nm. The cut-off size of the SMPS was 10 nm. The number
161 concentration in the size range of 3–10 nm was calculated as the difference in the total particle number
162 concentrations measured with uCPC and SMPS.

163 Total particle number concentrations measured on board the Cessna were first converted into standard
164 temperature and pressure conditions (273.15K, 1 atm) and then were corrected with the maximum
165 detection efficiency of the instrument based on laboratory calibrations. The maximum detection
166 efficiency of the PSM used in airborne measurement was 0.75 and that of uCPC was 0.99. The
167 maximum detection efficiencies of the PSMs used at the station were 0.8. Finally, the particle number
168 concentrations were corrected with respect to diffusional losses in the inlet part (Fig. 1) and inside
169 the sampling lines on the plane. The ground and tower data were assumed to have negligible inlet line
170 losses because of core sampling (Kangasluoma et al., 2016). The correction factor for the inlet part
171 was 0.716 for 1.5–3 nm particles and 0.720 for 3–10 nm particles based on simulation results using
172 COMSOL Multiphysics. Penetration efficiency through the sampling lines in the size range of 1.5–3
173 nm was 0.70 and in the size range of 3–10 nm 0.88.

174 All the results presented here are reported vertically as meters above the ground level, and all the data
175 were collected from within a distance of 30 km from the SMEAR II station in Hyytiälä. A typical
176 measurement flight includes a linear ascent from 100 m (a.g.l.) up to the FT region, 2500–3500 m,
177 and a descent back near to the canopy top level.

178 In this study, we analysed altogether 53 measurement profiles during 18 days. The flights were
179 conducted during three measurement campaigns: May-June 2015, August 2015 and April-May 2017,
180 either in the morning (7:00–12:00, UTC+2) or in the afternoon (12:00–15:00) time. The days were



181 classified as event, non-event or undefined days based on the NPF event classification method by Dal
182 Maso et al. (2005).

183 Well-mixed boundary layers are capped by a stable layer. The boundary layer height (BLH) was
184 visually estimated for each vertical measurement profile based on the particle number concentrations,
185 H₂O and CO₂ concentrations, potential temperature and relative humidity. When the sun is rising, the
186 mixing of air mass starts from near the ground, and aerosol particles originating from surface get
187 mixed upwards within the rising mixed layer. Inside the mixing layer, higher concentrations of H₂O
188 are sometimes seen when the turbulence mixes up the moisture from the surface. CO₂ tends to be
189 higher in the morning boundary layer due to respiration and decreases in the residual layer. The
190 vertical profile of the potential temperature is almost constant in the surface mixed layer and rapidly
191 increases with an increasing altitude under stable conditions.

192

193 2.4 Uncertainties

194 As described above, all the results were converted into STP-conditions and corrected for the
195 instrumental maximum detection efficiency and line losses according to the laboratory
196 characterizations of the flight setup. However, there are several factors causing uncertainties in the
197 measured concentrations. The flight speed, main flow rate, air pressure, relative humidity and
198 temperature are changing rapidly during a flight, which can cause variations in the inlet flows and the
199 performance of the instruments. It is poorly known how the uCPC and PSM behave under quickly
200 varying operational conditions. The reduced pressure at high altitudes may change the maximum
201 detection efficiency and cut-off size of laminar flow CPCs (e.g. Zhang and Liu, 1991; Herrman and
202 Wiedensohler, 2001). The pressure effect on the PSM cut-off size has been observed to be small (<
203 0.1 nm until 60 kPa) compared to the uncertainty caused by a changing relative humidity and particle
204 composition (Kangasluoma et al., 2016). Because of the uncertainties in the instrument cut-off sizes,
205 the true size range of the 1.5–3 nm concentration may vary with altitude and between different flights.
206 Because of the uncertainties in the determined concentrations, we should focus on the relative
207 behaviour of median values rather than absolute concentrations.

208

209

210



211 **3 Results and discussion**

212

213 The flight days were divided into event, non-event and undefined days based on the NPF event
214 classification by Dal Maso et al. (2005). Based on this classification on the ground level, the vertical
215 profiles of particles in the size ranges of 1.5–3 nm and 3–10 nm were studied separately in each type
216 of days. During event and undefined days, we also looked at differences between the morning and
217 afternoon times. The number of flights during non-event days is low (two vertical profiles), because
218 cloudiness makes the operation of the aircraft impossible. Non-event days are mostly cloudy in
219 Hyttiälä (Dada et al., 2017).

220 For the flight days, when we have comparable particle data from the ground station, we calculated
221 the median values of 1.5–3 nm particle concentration both inside BL on board the Cessna and on the
222 ground level. The boundary layer height was estimated for every vertical measurement profile.

223 **3.1 General features and vertical profiles**

224 The median values of particle concentrations, sensible heat flux (SHF) and estimated BLH was
225 calculated for the 27 cases when comparable data were available at the SMEAR II station (Table 1).
226 The values inside BL indicates here the observations on board Cessna, which means that the minimum
227 limit for altitude was around 100 m from ground level. The values on the ground level were measured
228 inside the forest canopy.

229 On average, we found that the concentration of 1.5–3 nm particles were higher inside the BL (1400
230 cm^{-3}) than on the ground station level (1100 cm^{-3}) (referred to from here as ‘ground’). The values
231 were the highest on NPF event days (1500 cm^{-3} inside BL and 1300 cm^{-3} on the ground) and undefined
232 days (1450 cm^{-3} inside BL and 1130 cm^{-3} on the ground) and clearly the lowest on non-event day
233 (890 cm^{-3} inside BL and 740 cm^{-3} on the ground) both inside the BL and on the ground level. It should
234 be noted that both of two non-event profiles were measured during the same afternoon in the spring
235 of 2015.

236 The observation of having somewhat lower concentrations of small particles at ground level is
237 probably due to higher sinks of particles and their precursors inside the canopy compared with above-
238 canopy air (Zha et al., 2017).

239 The median BLH of all the profiles was 1400 m, being lower in the morning (1100 m) and higher
240 during the afternoon flights (2000 m). Indicative of stronger vertical mixing, the median value of the



241 sensible heat flux (SHF) was the highest on the NPF event days, especially during the afternoon (286
242 W m^{-2}).

243 Figure 2 shows the median vertical profiles of the total particle number concentration in the size
244 ranges of 1.5–3 nm and 3–10 nm separately for the NPF event days, undefined days and one non-
245 event day. The profiles typically contain data from 100 m up to 2700 m above the ground level. It is
246 noticeable that non-event profile consists only two vertical profiles and both of them were measured
247 in the same afternoon. We found that airborne 1.5–3 nm particle concentrations were similar between
248 the event and undefined days, whereas substantially lower concentrations were observed on non-
249 event day. We also observed that during the event days there were clearly more 3–10 nm particles
250 inside BL than during undefined days (Fig. 2a and 2b). The reason for this could be that during the
251 undefined days the formation of sub-3 nm particles took place, yet the conditions were not suitable
252 for the particle growth to larger sizes (see Buenrostro Mazon et al., 2009; Kulmala et al., 2013). Our
253 findings are consistent with earlier observations of high sub-3 nm particle concentrations in Hyytiälä
254 on both event and undefined days compared with non-event days (Lehtipalo et al., 2009; Dada et al.,
255 2017).

256 During the NPF event days, median, 25th and 75th percentiles show that the concentration of sub-3
257 nm particles was relatively the highest right above the canopy top. This indicates that the sources of
258 particles and their precursor vapors are near the ground level. During the undefined days, the origin
259 of sub-3 nm particles was not necessarily at the ground level, as their concentration decreased right
260 before the ground level (from 100 m to 200 m). In addition, reviewing the median values in Table 1,
261 the concentration of 1.5–3 nm particles was observed to be higher inside the BL during morning times
262 of undefined days (2800 cm^{-3}) than during afternoon times (1150 cm^{-3}), oppositely to event days
263 (1070 cm^{-3} and 3020 cm^{-3} , respectively), which supports this hypothesis (Table 1). The concentrations
264 of both sub-3 nm and 3–10 nm particles were very low during the non-event days and we did not
265 observe any clear layers for these particles. However, it should be noted that our study included only
266 two such profiles, since the flight measurements were not possible to conduct during non-event days
267 due to meteorological conditions, especially cloudiness.

268 The measurement flights were conducted either in the morning (7:00–12:00, UTC+2) or in the
269 afternoon (12:00–15:00). We studied the median vertical particle concentrations separately for those
270 two times in order to estimate the effect of mixing strength on the vertical profile of particles on NPF
271 event and undefined days. As expected based on observed SHF fluxes, we found that the
272 concentrations of 1.5–3 nm particles inside the BL were, on average, most homogenous vertically
273 during the afternoons of the NPF event days (Fig. 3).



274 On NPF event days, we can see an interesting layer of 3–10 nm particles in the morning above the
275 BL at 2400 m. From this layer, the particles can mix down into the evolving BL. Similar behavior is
276 seen also on undefined days, when the increase in concentration of 1.5–3 nm particles is observed in
277 layer right below 2500 m in the morning and the particles are grown in size and mix downward until
278 afternoon.

279 **3.2 Diurnal variation of particle concentration at different altitudes in the lower** 280 **atmosphere**

281 We studied the median diurnal variation of total particle concentration (all particles > 1.5 nm) and
282 separately particle concentration in size range of 1.5–3 nm at different altitudes from around 100 m
283 to 2700 m above the ground level around the SMEAR II station area. The study included 17 vertical
284 measurement profiles during event days and 34 during undefined days. From Fig. 4a it can be seen
285 that the total particle number concentration over all measurement profiles was the highest near the
286 ground in the morning. The aerosol population mixed with cleaner air within the evolving BL after
287 the morning, which led to a decreasing particle number concentration, whereas the concentration
288 increased again towards the afternoon, presumably as a result of NPF. The highest particle number
289 concentrations were observed at 11:30–14:30 inside the BL, which coincides with the peak time of
290 NPF in Hyytiälä (Dada et al., 2018, in Prep.).

291 The sub-3 nm particle number concentrations (Fig. 4b) were the highest in the morning near the
292 ground level, with a second maximum around the noon. Later in the afternoon, sub-3 nm particle
293 concentration was clearly lower, probably because they apparently grew efficiently to larger sizes
294 and contributed significantly to the total particle concentration (Yli-Juuti et al., 2011). Both total
295 particles and sub-3 nm particles had the highest concentrations near the ground level throughout the
296 day, even though especially the total particle population seems to have been spread within the whole
297 mixed layer.

298 Figure 4c show the data availability for this analysis. It is noticeable that the number of data in each
299 100 m-half-an-hour cell varies considerably. In addition, one intense NPF event day with strong
300 particle formation in the early morning dominated the distribution due to the low number of flights at
301 around 7:00–8:00. Most of the data were collected either during the morning (8:30–11:30) or
302 afternoon (13:30–15:00). As we know, also the BLH, mixing of air and meteorological conditions
303 can differ significantly even within one day, and especially so between the NPF event and undefined
304 days.



305

306 **3.3 Case study – NPF in evolving BL**

307 The 13th of August 2015 was an intense NPF event day in Hyytiälä (Fig. 5a). During that day we
308 conducted two measurement flights around the SMEAR II station and observed the particle
309 concentration in size range of 1.5–3 nm to follow the development of BL and turbulent mixing (Fig.
310 6a, 6c, 7a, 7c). During the first measurement flight at 7:30–9:00, we observed a clear layer of 3–10
311 nm particles near the FT region above 2300 m. These particles were mixed down before the afternoon
312 flight, as this population was not anymore observed during that flight. The negative (downwards)
313 particle flux at SMEAR II after 12:00 supports this hypothesis (Fig. 5b).

314 The estimated BLH was ~700 meters during the first flight in the morning and had risen up to 1500–
315 1700 meters until afternoon flight. Below the FT, the vertical variation of the 1.5–3 nm particle
316 concentration was larger compared to the stable conditions in FT. The concentration of 1.5–3 nm
317 particles inside the BL increased during the morning flight (Fig. 6a and 6c) and decreased during
318 afternoon flight (Fig. 7a and 7c), whereas 3–10 nm particles seemed to behave in an opposite manner.
319 The sub-3 nm particle concentrations were clearly higher inside the BL than in the FT, and the
320 concentration increased towards the ground. This is consistent with organic vapors, emitted from the
321 ground vegetation, participating in NPF and growth (Kulmala et al., 2013; Ehn et al., 2014).

322

323 **4 Conclusions**

324

325 Small 1.5–3 nm particles were observed inside the convective BL on-board a Cessna aircraft. On
326 average, the highest concentrations of sub-3 nm particles were found during NPF event mornings
327 above the forest canopy top. This points towards the forest being an important source of the precursor
328 vapors for newly formed particles. Due to the convective mixing inside BL, small particles near the
329 ground started to mix up while sub-10 nm particles mixed down from the FT region. Strong vertical
330 mixing was more typical for the NPF event days than for the undefined and non-event days, especially
331 during the afternoon. The concentration of sub-3 nm particles was clearly higher inside the BL on
332 both NPF event days and undefined days compared with one non-event day, but their vertical
333 variation was somewhat different, reflecting the different mixing conditions. The event days also
334 showed a clear increase of 3–10 nm particles in the afternoon, which was missing on undefined days
335 when the NPF process had been interrupted.



336 We found that airborne and on-ground median concentrations of sub-3 nm particles were mostly in
337 good agreement. Some differences still existed, which can be explained by poor vertical mixing of
338 air, changes in air mass origins and regional variations. The concentrations of sub-3 nm particles on
339 the ground were, on average, somewhat lower than airborne observations, which indicates a higher
340 sink for these particles inside the forest canopy.

341

342 Acknowledgements

343 This work was supported by the European Research Council via ERC-Advanced Grant ATM-GTP
344 (742206), the European Commission via projects H2020-INFRAIA-2014-2015 project ACTRIS-2
345 (Aerosols, Clouds, and Trace gases Research InfraStructure), H2020 research and innovation
346 programme under grant agreement No 689443 (ERAPLANET) via project iCUPE (Integrative and
347 Comprehensive Understanding on Polar Environments), FP7 project BACCHUS (Impact of Biogenic
348 versus Anthropogenic emissions on Clouds and Climate: towards a Holistic UnderStanding, FP7-
349 603445), Academy of Finland via Centre of Excellence in Atmospheric Sciences (272041) and
350 NanoBiomass (307537).

351

352 References

353 Bianchi, F., Trostl, J., Junninen, H., Frege, C., Henne, S., Hoyle, C. R., Molteni, U., Herrmann, E.,
354 Adamov, A., Bukowiecki, N., Chen, X., Duplissy, J., Gysel, M., Hutterli, M., Kangasluoma, J.,
355 Kontkanen, J., Kuerten, A., Manninen, H. E., Muench, S., Perakyla, O., Petaja, T., Rondo, L.,
356 Williamson, C., Weingartner, E., Curtius, J., Worsnop, D. R., Kulmala, M., Dommen, J., and
357 Baltensperger, U.: New particle formation in the free troposphere: A question of chemistry and
358 timing, *Science*, 352, 1109–1112, 2016.

359 Buenrostro Mazon, S., Riipinen, I., Schultz, D.M., Valtanen, M., Dal Maso, M., Sogacheva, L.,
360 Junninen, H., Nieminen, T., Kerminen, V.-M. and Kulmala, M.: Classifying previously
361 undefined days from eleven years of aerosol-particle-size distribution data from the SMEAR II
362 station, Hyytiälä, Finland, *Atmos. Chem. Phys.*, 9, 667–676, 2009.

363 Chen, H., Hodshire, A.L., Ortega, J., Greenberg, J., McMurry, P.H., Carlton, A.G., Pierce, J.R.,
364 Hanson, D.R., Smith, J.N.: Vertically resolved concentration and liquid water content of
365 atmospheric nanoparticles at the US DOE Southern Great Plains site, *Atmos. Chem. Phys.*
366 *Discuss.*, doi.org/10.5194/acp-2017-586, 2017.



- 367 Crumeyrolle, S., Manninen, H., Sellegri, K., Roberts, G., Gomes, L., Kulmala, M., Weigel, R., Laj,
368 P. and Schwarzenboeck, A.: New particle formation events measured on board the ATR-42
369 aircraft during the EUCAARI campaign, *Atmos. Chem. Phys.*, Vol. 10, 14, 2010.
- 370 Dada, L., Paasonen, P., Nieminen, T., Buenrostro Mazon, S., Kontkanen, J., Peräkylä, P., Lehtipalo,
371 K., Hussein, T., Petäjä T., Kerminen, V.-M., Bäck, J. and Kulmala, M.: Long-term analysis of
372 clear-sky new particle formation events and nonevents in Hyytiälä, *Atmos. Chem. Phys.*, 17,
373 6227–6241, 2017.
- 374 Dada, L., et al.: Refined classification of atmospheric NPF and characterization of NPF event types
375 using air ion measurements, 2018, in Preparation.
- 376 Dal Maso, M., Kulmala, M., Riipinen, I., Wagner, R., Hussein, T., Aalto, P.P. and Lehtinen, K.E.J.:
377 Formation and growth of fresh atmospheric aerosols: eight years of aerosol size distribution
378 data from SMEAR II, Hyytiälä, Finland, *Boreal Env. Res.* 10: 323–336, 2005.
- 379 Ehn, M., Thornton, J. A., Kleist, E., Sipilä, M., Junninen, H., Pullinen, I., Springer, M., Rubach, F.,
380 Tillmann, R., Lee, B., Lopez-Hilfiker, F., Andres, S., Acir, I.-H., Rissanen, M., Jokinen, T.,
381 Schobesberger, S., Kangasluoma, J., Kontkanen, J., Nieminen, T., Kurtén, T., Nielsen, L. B.,
382 Jørgensen, S., Kjaergaard, H. G., Canagaratna, M., Maso, M. D., Berndt, T., Petäjä, T., Wahner,
383 A., Kerminen, V.-M., Kulmala, M., Worsnop, D. R., Wildt, J. and Mentel, T. F.: A large source
384 of low-volatility secondary organic aerosol, *Nature*, 506(7489), 476–479, 2014.
- 385 Hari P. and Kulmala M.: Station for Measuring Ecosystem-Atmosphere Relations (SMEAR II),
386 *Boreal Env. Res.* 10: 315–322, 2005.
- 387 Hermann, M. and Wiedensohler, A.: Counting efficiency of condensation particle counters at low-
388 pressures with illustrative data from the upper troposphere, *J. Aerosol Sci.*, Vol. 32, 8, 975–
389 991, 2001.
- 390 Kangasluoma, J., Franchin, A., Duplissy, J., Ahonen, L., Korhonen, F., Attoui, M., Mikkilä, J.,
391 Lehtipalo, K., Vanhanen, J., Kulmala, M. and Petäjä, T.: Operation of the Airmodus A11 nano
392 Condensation Nucleus Counter at various inlet pressures and various operation temperatures,
393 and design of a new inlet system, *Atmos. Meas. Tech.*, 9, 2977–2988, 2016.
- 394 Kerminen, V.-M., V.-M., Petäjä, T., Manninen, H.E., Paasonen, P., Nieminen, T., Sipilä, M.,
395 Junninen, H., Ehn, M., Gagné, S., Laakso, L., Riipinen, I., Vehkamäki, H., Kurten, T., Ortega,
396 K., Dal Maso, M., Brus, D., Hyvärinen, A., Lihavainen, H., Leppä, J., Lehtinen, K.E.J., Mirme,
397 A., Mirme, S., Hörrak, U., Berndt, T., Stratmann, F., Birmili, W., Wiedensohler, A., Metzger,



- 398 A., Dommen, J., Baltensperger, U., Kiendler-Scharr, A., Mentel, T.F., Wildt, J., Winkler, P.M.,
399 Wagner, P.E., Petzold, A., Minikin, A., Plass-Dülmer, C., Pöschl, U., Laaksonen, A. and
400 Kulmala, M.: Atmospheric nucleation: highlights of the EUCAARI project and future
401 directions, *Atmos. Chem. Phys.*, 10, 10829–10848, 2010.
- 402 Kerminen V.-M., Chen, X., Vakkari, V., Petäjä, T., Kulmala, M. and Bianchi, F.: Atmospheric new
403 particle formation: a review of observations, *Environ. Res. Lett.* (submitted).
- 404 Kulmala, M., Hämeri, K., Aalto, P.P., Mäkelä, J.M., Pirjola, L., Nilsson, E.D., Buzorius, G., Rannik,
405 Ü., Dal Maso, M., Seidl, W., Hoffman, T., Janson, R., Hansson, H.-C., Viisanen, Y., Laaksonen,
406 A. and O’Dowd, C.D.: Overview of the international project on biogenic aerosol formation in
407 the boreal forest (BIOFAR), *Tellus*, Vol. 53, 4, 2001.
- 408 Kulmala, M. and Kerminen, V.-M.: On the formation and growth of atmospheric nanoparticles,
409 *Atmos. Res.*, Volume 90, 2–4, 132–150, 2008.
- 410 Kulmala, M., Kontkanen, J., Junninen, H., Lehtipalo, K., Manninen, H.E., Nieminen, T., Petäjä, T.,
411 Sipilä, M., Schobesberger, S., Rantala, P., Franchin, A., Jokinen, T., Järvinen, E., Äijälä, M.,
412 Kangasluoma J., Hakala, J., Aalto, P.P., Paasonen, P., Mikkilä, J., Vanhanen, J., Aalto, J.,
413 Hakola, H., Makkonen, U., Ruuskanen, T., Mauldin, R.L., Duplissy, J., Vehkamäki, H., Bäck,
414 J., Kortelainen, A., Riipinen, I., Kurtén, T., Johnson, M.V., Smith, J.N., Ehn, M., Mentel, T.F.,
415 Lehtinen, K.E.J., Laaksonen, A., Kerminen, V.-M. and Worsnop, D.R.: Direct observations of
416 atmospheric aerosol nucleation, *Science* 339, 943–946, 2013.
- 417 Kulmala, M., Vehkamäki, H., Petäjä, T., Dal Maso, M., Lauri, A., Kerminen, V.-M., Birmili, W. and
418 McMurry, P.H.: Formation and growth rates of ultrafine atmospheric particles: A review of
419 observations, *J. Aerosol Sci.*, 35, 143–176, 2004.
- 420 Laakso, L., Gronholm, T., Kulmala, L., Haapanala, S., Hirsikko, A., Lovejoy, E. R., Kazil, J., Kurten,
421 T., Boy, M., Nilsson, E. D., Sogachev, A., Riipinen, I., Stratmann, F. and Kulmala, M.: Hot-air
422 balloon as a platform for boundary layer profile measurements during particle formation, *Boreal*
423 *Env. Res.*, 12, 279–294, 2007.
- 424 Lauros, J., Sogachev, A., Smolander, S., Vuollekoski, H., Sihto, S.-L., Mammarella, I., Laakso, L.,
425 Rannik, Ü. and Boy, M.: Particle concentration and flux dynamics in the atmospheric boundary
426 layer as the indicator of formation mechanism, *Atmos. Chem. Phys.*, 11, 5591–5601, 2011.



- 427 Lehtipalo, K., Sipilä, M., Riipinen, I., Nieminen, T. and Kulmala, M.: Analysis of atmospheric neutral
428 and charged molecular clusters in boreal forest using pulse-height CPC, *Atmos. Chem. Phys.*,
429 9, 4177–4184, 2009.
- 430 Mirme, S., Mirme, A., Minikin, A., Petzold, A., Hörrak, U., Kerminen, V.-M. and Kulmala, M.:
431 Atmospheric sub-3 nm particles at high altitudes, *Atmos. Chem. Phys.*, 10, 437–451, 2010.
- 432 O’Dowd, C., Yoon, Y., Junkermann, W., Aalto, P., Kulmala, M., Lihavainen, H., and Viisanen, Y.:
433 Airborne measurements of nucleation mode particles II: boreal forest nucleation events, *Atmos.*
434 *Chem. Phys.*, 9, 2009.
- 435 Platis, A., Altstädter, B., Wehner, B., Wildmann, N., Lampert, A., Hermann, M., Birmili, W. and
436 Bange, J.: An observational case study on the influence of atmospheric boundary-layer
437 dynamics on new particle formation, *Boundary-Layer Meteorol.*, Vol. 158, 1, pp. 67–92, 2016.
- 438 Rannik, Ü., Petäjä, T., Buzorius, G., Aalto, P., Vesala, T. and Kulmala, M.: Deposition Velocities of
439 Nucleation Mode Particles into a Scots Pine Forest, *Environ. Chem. Phys.*, 22, pp. 97–102,
440 2000.
- 441 Schobesberger, S., Väänänen, R., Leino, K., Virkkula, A., Backman, J., Pohja, T., Siivola, E.,
442 Franchin, A., Mikkilä, J., Paramonov, M., Aalto, P. P., Krejci, R., Petaja, T. and Kulmala, M.:
443 Airborne measurements over the boreal forest of southern Finland during new particle
444 formation events in 2009 and 2010, *Boreal Env. Res.*, 18, 145–163, 2013.
- 445 Siebert, H., Stratmann, F. and Wehner, B.: First observations of increased ultrafine particle number
446 concentrations near the inversion of a continental planetary boundary layer and its relation to
447 ground-based measurements, *Geophys. Res. Lett.*, Vol. 31, Issue 9, 2004.
- 448 Stull, R. B.: An introduction to boundary layer meteorology, Springer Science & Business Media,
449 2012.
- 450 Vanhanen, J., Mikkilä, J., Lehtipalo, K., Sipilä, M., Manninen, H., Siivola, E., Petäjä, T., and
451 Kulmala, M.: Particle size magnifier for nano-CN detection, *Aerosol Sci. Tech.*, 45, 2011.
- 452 Väänänen, R., Krejci, R., Manninen, H.E., Manninen, A., Lampilahti, J., Buenrostro Mazon, S.,
453 Nieminen, T., Yli-Juuti, T., Kontkanen, J., Asmi, A., Aalto, P.P., Keronen, P., Pohja, T.,
454 O’Connor, E., Kerminen, V.-M., Petäjä, T. and Kulmala, M.: Vertical and horizontal variation
455 of aerosol number size distribution in the boreal environment, *Atmos. Chem. Phys. Discuss.*,
456 doi:10.5194/acp-2016-556, 2016.



- 457 Wehner, B., Siebert, H., Stratmann, F., Tuch, T., Wiedensohler, A., Petäjä, T., Dal Maso, M. and
458 Kulmala, M.: Horizontal homogeneity and vertical extent of new particle formation events,
459 *Tellus*, Vol. 59, 3, 362–371, 2007.
- 460 Wehner, B., Wehner, F., Ditas, F., Shaw, R.A., Kulmala, M. and Siebert, H.: Observations of new
461 particles formation in enhanced UV irradiance zones near cumulus clouds, *Atmos. Chem.*
462 *Phys.*, 15, 11701–11711, 2015.
- 463 Wehner, B., Siebert, H., Ansmann, A., Ditas, F., Seifert, P., Stratmann, F., Wiedensohler, A.,
464 Apituley, A., Shaw, R., and Manninen, H. E.: Observations of turbulence-induced new particle
465 formation in the residual layer, *Atmos. Chem. Phys.*, 10, 4319–4330, 2010.
- 466 Yli-Juuti, T., Nieminen, T., Hirsikko, A., Aalto, P.P., Asmi, E., Hörrak, U., Manninen, H.E.,
467 Patokoski, J., Dal Maso, M., Petäjä, T., Rinne, J., Kulmala, M. and Riipinen, I.: Growth rates
468 of nucleation mode particles in Hyytiälä during 2003–2009: variation with particles size,
469 season, data analysis method and ambient conditions, *Atmos. Chem. Phys.*, 11, 12865–12886,
470 doi:10.5194/acp-11-12865-2011, 2011.
- 471 Zha, Q., Yan, C., Junninen, H., Riva, M., Aalto, J., Quéléver, L., Schallhart, S., Dada, L., Heikkinen,
472 L., Peräkylä, O., Zou, J., Rose, C., Wang, Y., Mammarella, I., Katul, G., Vesala, T., Worsnop,
473 D.R., Kulmala, M., Petäjä, T., Bianchi, F. and Ehn, M.: Vertical characterization of highly
474 oxygenated molecules (HOMs) below and above a boreal forest canopy, *Atmos. Chem. Phys.*
475 *Discuss.*, doi.org/10.5194/acp-2017-1098, 2017.
- 476 Zhang, Z. Q. and Liu, B. Y. H.: Performance of Tsi 3760 Condensation Nuclei Counter at Reduced
477 Pressures and Flow-Rates, *Aerosol Sci. Tech.*, 15, 228–238, 1991.
- 478
- 479

480 **Tables**

481

482 Table 1. Numerical statistics about boundary layer height (BLH) and sensible heat flux (SHF)
 483 indicating the mixing of air mass, and concentrations of 1.5–3 nm particles during measurement
 484 flights in 2015 and 2017. The morning flights have been conducted between 7:00–12:00 o'clock and
 485 afternoon flights at 12:00–15:00 o'clock. The low number of flights during non-event days is caused
 486 by the cloudiness which makes the operation of the aircraft impossible.

487

	Number of flight profiles	Median conc. (1.5–3 nm) inside BL [cm ⁻³]	Median conc. (1.5–3 nm) on ground level [cm ⁻³]	Median BLH [m]	Median SHF [W m ⁻²]
All days	27	1404	1104	1400	192.3
morning	13	1995	888	1100	174.6
afternoon	14	1232	1251	2000	220.5
Events	11	1509	1300	1250	200
morning	6	1066	950	800	154.5
afternoon	5	3019	1435	1550	285.8
Undefined	14	1450	1129	1450	180.7
morning	7	2793	838	1200	182.6
afternoon	7	1149	1169	2000	178.7
Non-events	2	887	744	2000	162.3
morning	-	-	-	-	-
afternoon	2	887	744	2000	162.3

488

489

490

491

492

493

494

495

496

497

498

499

500



501 **Figures**

502

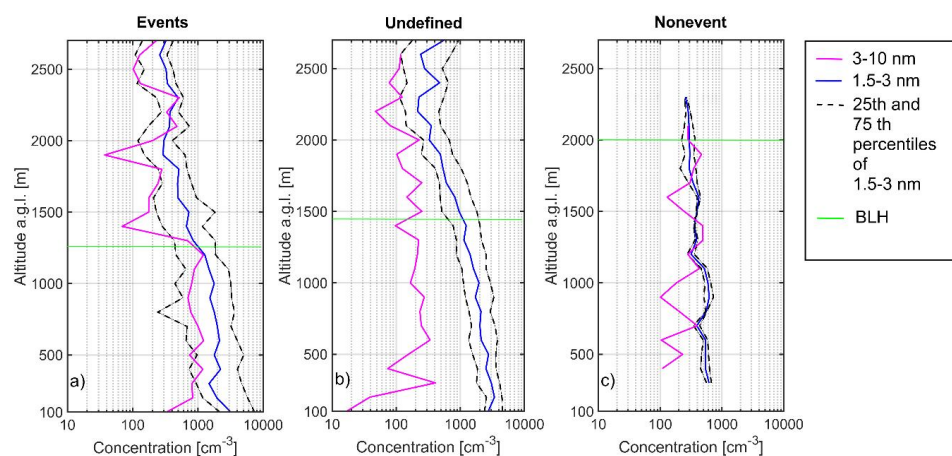


503

504

505 Figure 1. Instrumentation rack was installed inside the cabin (on the left) and the sample air for the
506 instrumentation was taken from a steel tube at 50 cm distance from the fuselage of the plane (on the
507 right).

508

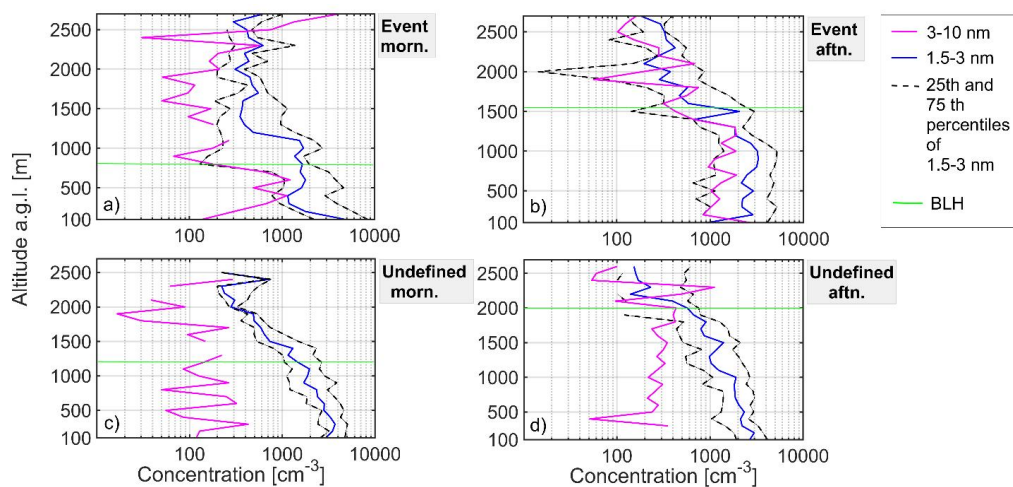


509

510

511 Figure 2. All day median particle concentrations in two size ranges, 3–10 nm (pink) and 1.5–3 nm
512 (blue) and 25- and 75-percentiles (dashed lines) of the 1.5–3 nm particle concentration, as a
513 function of altitude over 17 event day (a), 34 undefined day (b) and 2 non-event day afternoon
514 profiles (c). The concentrations were calculated from the differences between three instruments
515 (PSM, uCPC and SMPS) at different cut-off sizes: 1.5 nm, 3 nm and 10 nm, respectively. The data
516 were collected from near (< 30 km) to SMEAR II station during spring and August flight
517 measurement campaigns in 2015 and spring campaign 2017. Median boundary layer heights are
518 marked by green lines.

519



520

521

522 Figure 3. Median concentrations in two size ranges (1.5–3 nm and 3–10 nm) and 25- and 75-
523 percentiles of 1.5–3 nm particle concentration over measurement profiles during event and
524 undefined days separately for morning (a, c) (7:00–12:00 o'clock) and afternoon (b, d) (12:00–
525 15:00 o'clock) times. The median vertical profiles were defined over 9 event morning, 8 event
526 afternoon, 18 undefined morning and 16 undefined afternoon profiles. Median boundary layer
527 heights are marked by green lines.

528

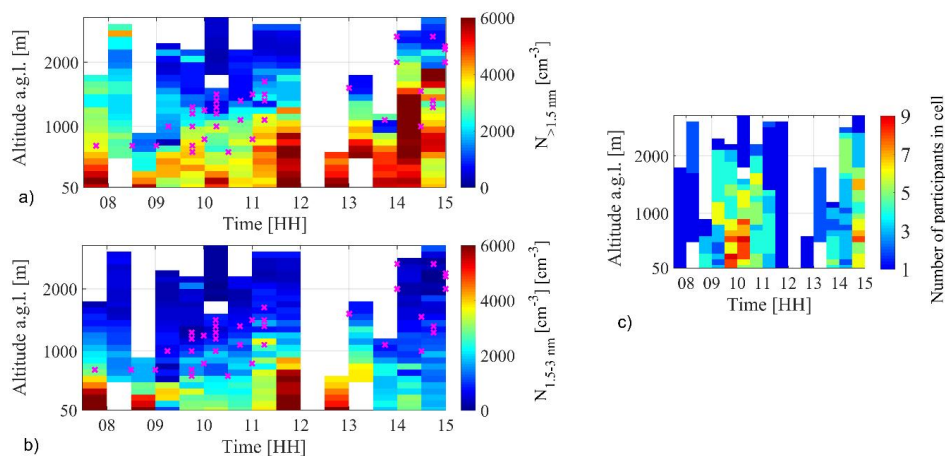
529

530

531

532

533



534

535

536 Figure 4. Panel a) shows median total particle number concentration at different altitudes calculated
537 over 51 measurement flight profiles (17 event day and 34 undefined day profiles) during 2015
538 spring and August and 2017 spring campaigns in 30 km maximum distance from SMEAR II station.

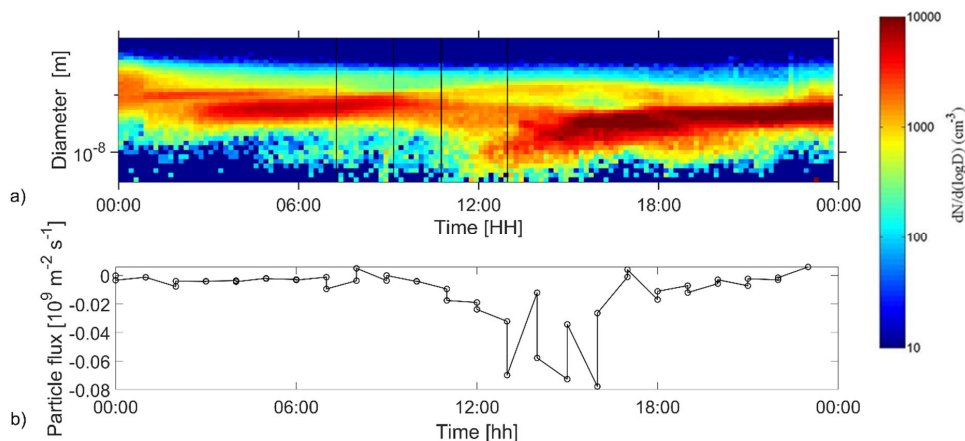
539 The total particle number concentration was measured with PSM with the cut-off size of 1.5 nm.

540 Colour scale indicates total number concentration. Panel b) shows median particle number
541 concentration in the size range of 1.5–3 nm at different altitudes. The value is defined as difference
542 of total number concentrations with different cut-off sizes; PSM (1.5 nm) and uCPC (3 nm). Panel
543 c) shows the number of data points in each cell of figures a-b). Estimated boundary layer heights are
544 marked as crosses in figures a-b) over flight profiles. Each cell includes the median value of all
545 measurement points inside the 100 m bin and half-an-hour.

546

547

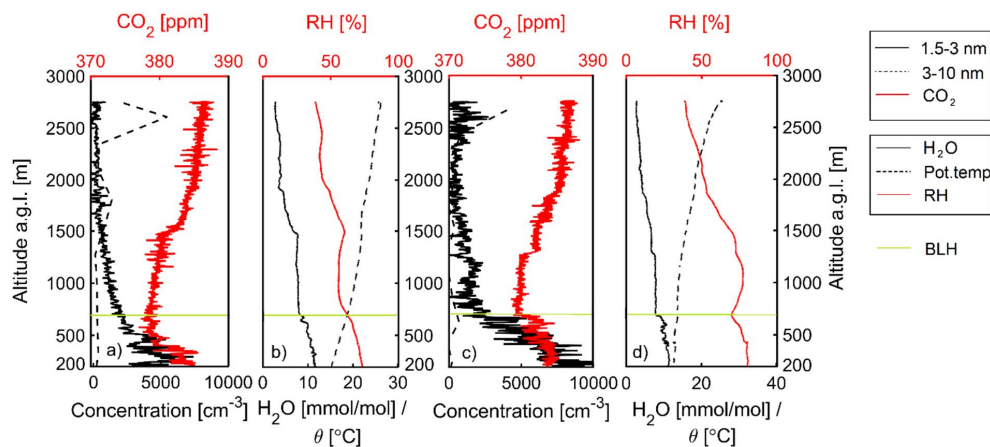
548



549

550 Figure 5. New particle formation event at SMEAR II station in Hyytiälä on 13th August 2015. Panel
 551 a) shows the number size distribution measured by Differential Mobility Particle Sizer at ground
 552 level inside the forest canopy. Start and end times of two measurement flights were marked by
 553 vertical lines in figure. Panel b) shows the particle flux measured at 23 m above ground level at the
 554 station. Negative particle flux indicates particles flux downwards.

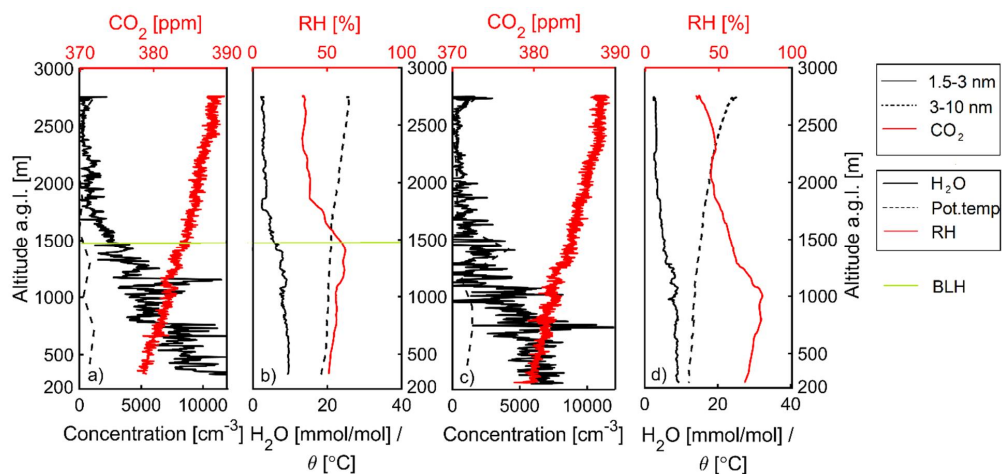
555



556

557 Figure 6. Vertical profiles during the first measurement flight at 7:30–9:00 a.m. on 13th August
 558 2015 (marked in Fig 5). Panels a, b) show data from the ascent and c, d) from the descent. Figures
 559 a) and c) show the number concentration of 1.5–3 nm (black solid line) and 3–10 nm (dashed line)
 560 particles and the carbon dioxide concentration (red). Panels b) and d) show water vapor
 561 concentration (black), relative humidity (red) and potential temperature (dashes line) profiles. The
 562 green line is the estimated boundary layer height.

563



564

565 Figure 7. Measurement profiles like in the previous figure, but during the second measurement
566 flight on 13th August 2015 at 11:00 a.m. – 12:45 p.m.